Science and Engineering Research Council
Rutherford Appleton Laboratory
CHILTON, DIDCOT, OXON, OX11 0QX

RAL-87-019

The Charge Sensitive Pre-amplifier used for Photo-Triode Readout in the OPAL Lead Glass Detector

R Stephenson

March 1987

Science and Engineering
Research Council

RAL 87-019

THE CHARGE SENSITIVE PRE-AMPLIFIER USED FOR VACUUM PHOTO-TRIODE READOUT IN THE OPAL LEAD GLASS DETECTOR.

R. Stephenson.

ABSRACT

This report describes the preamplifiers which have been developed specifically to process the signals from the vacuum photo-triodes used on the OPAL experiment at CERN. It outlines the design philosophy, decribes the chosen circuit arrangement and includes performance test data. It includes details of the surface mount manufacturing process used for the 2264 production amplifiers, and describes the automated acceptance testing system used to individually check their performance.

March 87

INDEX

INTRODUCTION

The electro-magnetic calorimeter of the OPAL experiment (CERN) consists of an array of lead glass scintillator elements arranged to provide almost complete 4 pi coverage around the interaction point of the electron and positron beams. Each block is fitted with a photo-tube to detect the photons and is provided with an individual ADC channel. The barrel part of the detector is instrumented using conventional photo-multiplier tubes, but since the end caps are located within the solenoidal magnetic field these are instrumented using specially developed vacuum photo-triodes (VPT's) which are magnetic field tolerant.[1] The VPT's are single stage photo-multipliers with an electron gain of around 10, in contrast with the 10^3 to 10^6 gain expected of normal photo-multipliers. The preamplifiers replace the gain of the missing multiplier stages, while maintaining a similar noise performance to that of a normal photo-multiplier.

The preamplifier is of the form shown in figure (1). The input stage is configured as a charge sensitive amplifier by applying feedback via a small capacitance C_f around a high gain inverting amplifier stage. All the current flowing in the input terminal flows into C_f, the operational amplifier adjusting the potential of its output to maintain the virtual earth point at zero as the current charges the feedback capacitor. With a C_f of 1 pF the charge sensitivity of this stage is 1 volt / pico coulomb, or 160 nano-volts per electron. R_f provides a discharge path for the charge collected in C_f. The input impedance of this stage is equivalent to a capacitor given by (C_f X A), where A is the operational amplifier gain. With A typically > 10^4, the source sees a capacitance of > 10 nF at the amplifier input terminals. If the source is itself capacitive then the source charge is shared between C_s and C_{in} in the ratio of their values. With C_{in} >10 nF, the proportion of the total input charge deposited in C_s is negligable for practical values of C_s. This results in the charge sensitivity being independant of the input shunt capacitance C_s. The finite shunt capacitance of the source does have several undesirable effects however:-

a/ The voltage noise present at the amplifier input is amplified by a factor 1 + (C_s / C_f), since the voltage noise appears in series with the operational amplifier input, and this is equivalent to driving the non-inverting input from an identical noise source, see figure (2).

b/ The VPT capacitance stores a charge of approximately 3 * 10^{-8} C when working at 1200 volts. This energy is sufficient to cause serious damage to the preamp front end should the VPT break down, or be exposed to a sudden large light source. The preamp must incorporate suitable input protection.

c/ Any ripple voltage present on the VPT bias voltages will be amplified by a factor (C_s / C_f) since the preamplifier performs as a virtual earth voltage amplifier with the input and feedback resistances replaced by capacitors. To acheive a noise contribution at the amplifier output due to ripple which is equivalent to < 5

electrons RMS (2 % approx), the EHT ripple must be < 20 nV RMS at all frequencies within the amplifier pass band (for C_s equals 40 pF). The ripple filter must have a reciprocal response to the amplifier L.F. response to maintain constant overall ripple attenuation down to low frequencies.

d/ Any modulation of the inter-electrode capacitances of the VPT will result in a flow of charge in the amplifier input since the applied voltage is fixed. The VPT's internal assembly exibits high "Q" mechanical resonances at frequencies within the audio range, and these can readily be excited by vibration or air borne noise. The primary resonance present in the Phillips tubes used on OPAL is around 300 Hz. Experiment has shown that to ensure good noise immunity from this source , the amplifier response must be > 80 db down at 300 Hz relative to the mid band level. [2]

Charge amplifiers are generally used with shaping amplifiers which tailor the frequency response to give optimum signal to noise ratio. The best noise performance is obtained from the amplifier when its bandwidth is minimised to minimise the noise, consistant with allowing the signal to reach its peak value and stay there for the duration of the measurement gate. This implies both high and low pass filter stages carefully adjusted for optimum performance. A typical amplifier of this type would will exhibit noise equivalent to around 140 electrons RMS with the input open circuit and an optimal filter.[3]

The preamp for use with the OPAL VPT's has constraints on choice of filter time constants which result in some degradation from the ultimate noise performance. These constraints are :-

a/ LEP will produce a beam crossing every 22 micro-seconds. To ensure that the system has time to settle between events, the lower cut-off must have a time constant of < 4 micro seconds. This allows 5 time constants for recovery, during which the signal will decay to < 1% of its peak value. The probability of having significant hits in the same channel on consecutive machine cycles makes 1% an acceptable figure.

b/ The requirement for the response to be 80 db down at 300 Hz to avoid VPT microphonics effects, along with the required recovery time constant of around 4 micro seconds dictates that the lower cut off filter be second order. The arrangement chosen has 2 stages each with approximately 3 micro second time constants, this gives a lower -3 db point of approximately 50 KHz and a slope of 12 db / octave, ie. -83 db at 300 Hz.

c/ The choice of the high cut filter characteristic is a compromise between rise-time and noise. A fast rise-time will allow the output pulse to reach peak amplitude quickly, before any decay due to the low cut filter has become significant. For minimum noise however, the noise bandwidth should be minimised. These conditions are mutually exclusive, also the gate width of the ADC is another variable in the argument. A compromise has been reached in this design which allows an upper -3 db point of 350 KHz, which gives optimum noise performance when the ADC gate is 2 micro seconds long.

The amplifier is required to drive an ADC located 30 metres away with high precision. To acheive this, a balanced cable system is required, with a balanced to unbalanced conversion located close to the ADC. This conversion is best performed using a purpose designed pulse transformer to provide the matching and break any earth loops. The second stage of low cut filtering is also provided close to the ADC. The predicted dynamic range of the signals is 2 * 10^3, and this sets the gain of the shaping amplifier at X 15 to give signal levels on the cables in the range +/- 1 mV to +/- 2 volts. This range of signal level was chosen as a compromise between noise pick-up at low level and excessive drive requirements at high levels. A resistive attenuator is fitted after the transformer to adjust the levels at the ADC input.

Optimum noise performance in a charge amplifier is achieved when the discharge resistance R_f is as large as possible. The limit on its value is set by the mean current flowing into to the amplifier input. The largest component of the amplifier input current is the VPT dark current which for the OPAL tubes has a maximum acceptable value of 5 nA. This current flows in R_f causing an IR drop, and displacing the working point at the amplifier output. The value of R_f has been set at 200 Meg-ohms which gives a worst case working point displacement of 1 volt.

The preamplifier was built as a sub assembly which mounts on a circular mother board carrying the EHT decoupling and input protection components. By using the surface mounting assembly technique for the preamplifier its physical size was reduced to 18 X 40 mm with a 0.1 inch pitch SIL connector along one long edge.

CIRCUIT DESCRIPTION

Figure (3) shows the complete wiring diagram for the signal system up to the ADC input, including the internal circuit diagram of the pre-amplifier.

The preamplifier input amplifier is formed by TR1, TR2 and TR3. TR1 is a junction FET common source stage, operating with an I_{drain} of 10 mA, providing a gm of typically 15 mA/volt. R1 forms the load resistor, giving a typical voltage gain of 10. TR2 reduces the output impedance of the first stage by providing current gain, and drives the signal into the emitter of the common base stage TR3. TR3 provides a large voltage gain defined by the ratio of the collector and emitter impedances. The collector impedance is a combination of the transistor output impedance, IC1's input impedance and the dynamic impedance of the current regulator diode D2. This gives a typical load impedance of > 10^5 ohms. The emitter impedance consists of R1 divided by the current gain of TR2, plus the r_e's of TR2 and TR3. D2 sets the quiescent current at 330 micro-amps which gives an r_e of 75 ohms. Hence the total emitter resistance is typically 160 ohms, and the gain of the TR3 stage approaches 10^3. Hence the open loop gain of the complete input stage is approaching 10^4. Feedback is provided by C1, while R2 provides a discharge path for C1 and applies the DC bias to TR1 gate to maintain the working point.

IC1 forms the shaping amplifier and provides one half of the balanced output drive, while IC2 is a unity gain inverting stage providing the other half of the balanced output drive. The voltage gain of IC1 is set at 30 by R6 and R8. The H.F. roll-off is defined by C7 and R8, giving a break frequency of 194 KHz and a slope of 6 db per octave.

The arrangement chosen for IC2 was adopted as it provides freedom from latch-up on overload when driving highly capacitive loads, when large currents may flow in the input protection diodes of the NE5534's. The values chosen for R9 and R10 set the gain of IC2 to provide the correct output amplitude from the inverting stage in this arrangement. C10 provides a bandwidth limit on IC2, to reduce the noise contribution from this source.

The gain and bandwidth control components are connected via external links which allow external components to be substituted to obtain different values. The internally set gain of 30 combined with the HF roll-off at 194 KHz come close to the gain bandwidth product of the NE5534 of 10 MHz. Working close to the GBW results in a lower noise contribution from the later stages of the operational amplifiers.

The L.F. roll-off is controlled by C4 and R6, giving a break frequency of 48.229 KHz, with 6 db per octave slope. It was intended that the second stage of L.F. roll-off would be provided by the output matching transformer. This was eventually abandoned because current spikes associated with amplifier overloads at switch-on or when over-driven changed the transformer characteristics, resulting in changes in the overall gain. In the final arrangement the second high pass filter is provided by a capacitor in series with the ADC input.

IC's 1 and 2 are DC coupled to the input stage and transfer the TR1 gate bias voltage to the output pins under quiescent conditions. This is a useful diagnostic since this value can be checked remotely.

Input protection is provided by the gate source junction of TR1 for + ve spikes and by D1 for - ve spikes. (D1 can be disconnected in applications requiring the lowest noise at the expense of input protection). Additional protection is provided externally by a clamp consisting of pairs of diodes and transistors, where the diodes act as 0.6 volt reference devices, turning on the clamp transistors for either polarity. This clamp is AC coupled to the input line to prevent leakage current introducing shot noise. Initial tests were conducted with the VPT anode connected directly into the preamp input with the transistor / diode network in parallel. Simulated breakdown tests produced fault currents in excess of 70 Amps in the protection network, resulting in device damage. Larger devices result in larger junction capacitances and hence increased noise, so a resistor was added in series with the VPT input to limit the fault current. The resistor is by-passed at low frequencies by an inductor, which attenuates the Johnson noise of the resistor within the amplifier pass band, but which blocks the fast edge produced by an EHT breakdown in the VPT. The choke is air cored to avoid core saturation at high currents and is wound on the body of the resistor.

EHT ripple filtering is provided by a 2 stage low pass filter. The first stage is formed by a 22 Meg resistor in the interface and the 3000 pF shunt capacitance of the 30 metres of RG174U coaxial connecting cable. This stage has a turn-over frequency of 2.4 Hz. The second stage is provided within the VPT housing, with a turn-over frequency of 7.2 Hz. The 2 stages produce a combined attenuation of around 50 db @ 50 Hz and of 154 db at 20 KHz, the likely invertor frequency of the EHT supplies. An EHT supply with 1 volt RMS of ripple at 20 KHz would produce 33 nV RMS of ripple at the VPT. Taking the gain and filtering characteristics of the amplifier into account, this would result in a noise signal at the amplifier output equivalent to 2 or 3 electrons RMS.

The overall gain of the system is set by a resistive attenuation network located after the transformer. The ADC input impedance is 50 ohms, but it requires a source impedance > 150 ohms for satisfactory noise performance. This requirement is met by the series resistor at the network output, which additionally provides some signal attenuation. The cable is matched by a 1 : 1 transformer with a nominal 100 ohm load. This load is formed by an 82 ohm series resistor and a plug-in gain setting shunt resistor together with the ADC circuit in parallel. The overall attenuation is set by adjusting the plug-in shunt resistor over a range of 4 : 1.

PREAMPLIFIER PERFORMANCE

For performance testing the preamplifier was mounted in a screened box with decoupled D.C. supplies, with input charge delivered via a 1 pF capacitor, and the output signal taken via a 1.414 to 1 transformer to match the 100 ohm balanced output to 50 ohms.

The measured overall sensitivity of the preamp is 0.85 micro-volts peak / electron into 50 ohms. Figure (4) shows the variations in sensitivity with ambient temperature. Figure (5) shows the variation in sensitivity as the source shunt capacitance is varied. The sensitivity is reduced to 50 % with an input shunt capacitance of around 10 nF, hence the effective input capacitance is around 10 nF.

Figure (6) shows the maximum available output before saturation of approximately 3 volts peak into 100 ohms differential at the amplifier output, or 2 volts into 50 ohms after the transformer. Figure (7) shows the variation in output pulse risetime as the source shunt capacitance is varied. No significant change is noted for practical values of source shunt capacitance since the risetime is dominated by the shaping amplifier low pass filter characteristic.

Noise measurements were made using an integrating ADC in CAMAC driven by an Apple micro-computer. Input signals corresponding to 1 * 10^4 electrons, and 2 * 10^4 electrons were injected into the input using a 1 pF capacitor and a known voltage step. The corresponding outputs from the preamplifier were fed to the ADC via a matching transformer and high pass filter network, and the magnitudes of the individual events were histogrammed. Subtracting the peak values corresponding to the 2 input levels gives a sensitivity calibration

free from offset effects, while measuring the FWHM values of the peaks gives the system noise which can be expressed directly in electrons. This noise contains the pulse generator and ADC noise in addition to the preamp noise. Careful choise of signal levels ensured that the preamplifier noise was the dominant noise source.

Figure (8) shows the variation in observed noise as the source shunt capacitance is varied for a typical preamp. This was acheived by adding a shunting capacitor at the preamp input. These measurements were taken with the internal protection diode connected, but without any additional external network. The ADC gate width was set at 2 microseconds for these tests. The noise level with the input open circuit corresponds to 175 electrons RMS, increasing by an additional 4 to 5 electrons RMS per pF of shunt capacitance.

The measured noise is a function of the filter characteristics and the ADC gate width. Figure (9) shows a plot of the gate width dependance using the final values of filter parameters. 2 micro-seconds is close to optimum.

The source of the noise is almost entirely in the first stage. Figure (10) shows a spectrum analyser plot of the amplifier output. The shape of the curve closely follows the shaping amplifier's filter characteristic. Repeating the measurement with TR3 collector decoupled to ground to remove the first stage noise results in a noise spectrum 20 dB quieter indicating that the shaping amplifier's noise contribution is insignificant.

The choice of shaping amplifier filter characteristic, the cable matching and attenuating network parameters and the ADC gate width are a compromise between noise performance and the need to be ready to receive the next event 22 micro-seconds later. Figure (11) shows the output waveform from the matching and attenuating network which feeds the ADC. The waveform has recovered to < 1% of its peak value 22 micro-seconds after the event.

Tests to simulate an EHT breakdown in the VPT were carried out using an EHT relay to discharge a 2 nF capacitor charged to 1200 volts into the preamplifier input. This was repeated at 15 second intervals for periods of > 1 hour with no apparent damage to either the protection network or the preamplifier. The capacitance of the protection components does result in an increase in the total noise of the preamplifier of approximately 15 electrons RMS.

The quiescent circuit power dissipation is divided between the +ve and -ve power rails as follows :-

+12 volts	18 mA	216 mW
-12 volts	8 mA	96 mW
	Total Power	312 mW

MANUFACTURE and TEST

The preamplifiers were constructed using the surface mount construction technique on a printed circuit board produced from convential GRP material. All the components with the exception of D1 and D2 were available in small outline packages, all components except these were fitted using solder paste and a vapour phase soldering machine. D1 and D2 were then fitted by hand.

The layout was arranged to be single sided with no through board "via's", with 14 connecting pins on 0.1 inch pitches arranged along one long edge. A gap was left between pins 5 and 6 for connector polarisation.

Figure (12) shows a typical production preamplifier.

Once assembled, the preamplifiers were given a quick test at the manufacturers using a purpose built test unit which checked that both outputs were working in response to a standard test input. The preamplifiers were then loaded in batches of 32 into a computer driven automatic test system where the gain and noise characteristics of each preamplifier were measured. In this system the preamp input was driven with a repetitive charge signal of 1 * 10^4 electrons. The resulting preamp output was measured using a charge sensitive ADC and the spread of output amplitudes were histogrammed in the computer memory. The mean and the full width at half maximum (FWHM) values were evaluated, then the process was repeated at an input level of 2 * 10^4 electrons. Values for the gain and noise of the preamplifier were calculated and filed on floppy disc. The process was then repeated on the next preamplifier until all 32 had been tested. This process took approximately 3 hours, and was carried out fully automatically by an Apple 2 computer. The preamplifier in channel 1 was not changed throughout the whole testing period to allow the calibration of the measuring system to be standardised.

The production cost of the 2500 preamps was 12 pounds each, including all components and the manufacturers quick test. All the preamplifiers delivered by the manufacturer worked, figure (13) shows the spread in the noise performance of all the preamps.

The tested preamps were graded by noise performance and fitted to mothercards populated with all the decoupling and protection circuits. These mothercards were coated with a conformal coating laquer, then fitted into complete base assemblies. The VPT's were tested independently, graded by performance and paired up with suitable amplifiers. The VPT's were then fitted into the housings and a performance check carried out. Finally the VPT was bonded to its glass block and the complete assembly fitted into its brass outer tube. A further series of tests and calibration measurements was then carried out, all the data being stored in a computer data-base.

Figure (13) shows a typical assembly with VPT fitted ready to be attached to its glass block.

CONCLUSION

Providing a preamplifier to restore the gain of a vacuum photo-triode to that expected of a normal photo-multiplier proved a demanding task. Building a photo-tube housing assembly to house the tube and amplifier also proved more difficult than housing a normal photo-tube. By designing a preamplifier specifically for this application, the overall performance has been optimised, while the circuit complexity has been minimized. Use of a surface mounted preamplifier sub-assembly aided testing and construction, and probably improved the overall consistancy of the final product.

Overall, the vacuum photo-triode / preamplifier combination provides a stable photo-detector for the OPAL lead glass calorimeter which meets the performance specification requirements at a reasonable cost.

ACKNOWLEDGEMENTS

The author would like to acknowledge the contributions made by Mr S.R. Burge and Mr J.E. Simmons of the P.A.G. Electrical design section during the design and production stages, and the members of the P.A.G. Electrical test section who were involved in the testing programme.

REFERENCES

1/ A Photo-triode instrumented lead glass calorimeter for use in a strong magnetic field in OPAL.

P.W. Jefferies et al, RAL 85-058

2/ Tests on a low noise charge sensitive amplifier used in conjunction with a vacuum phototriode.

R. Stephenson, RAL 83-075

3/ A low noise charge sensitive amplifier for use in vacuum photo diode readout.

R. Stephenson, RAL82-082

List of Diagrams

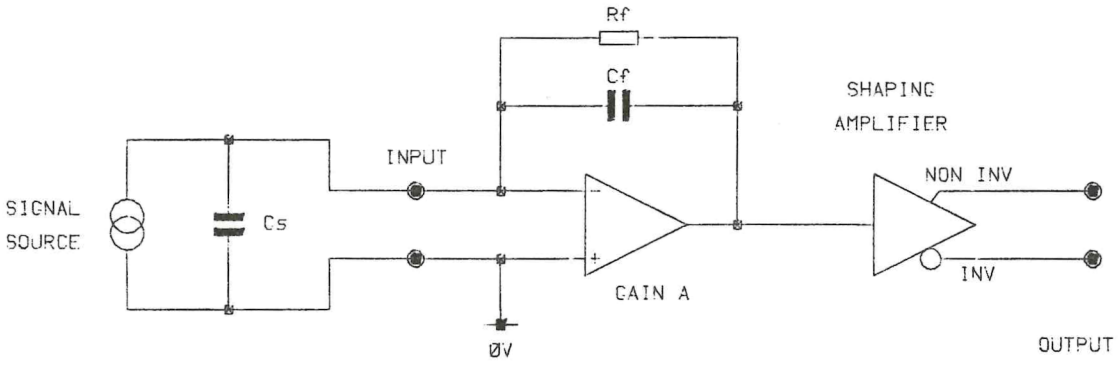

FIGURE 1

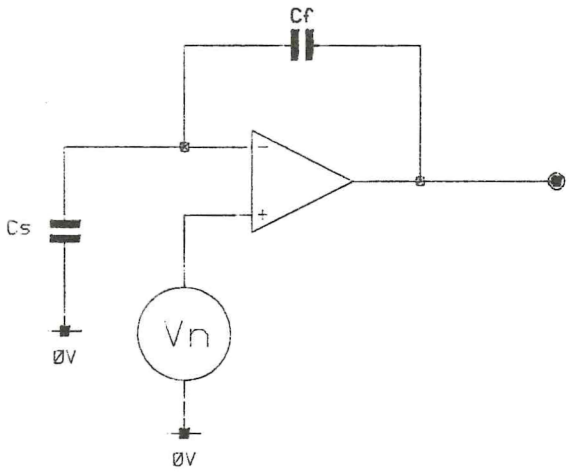

FIGURE 2

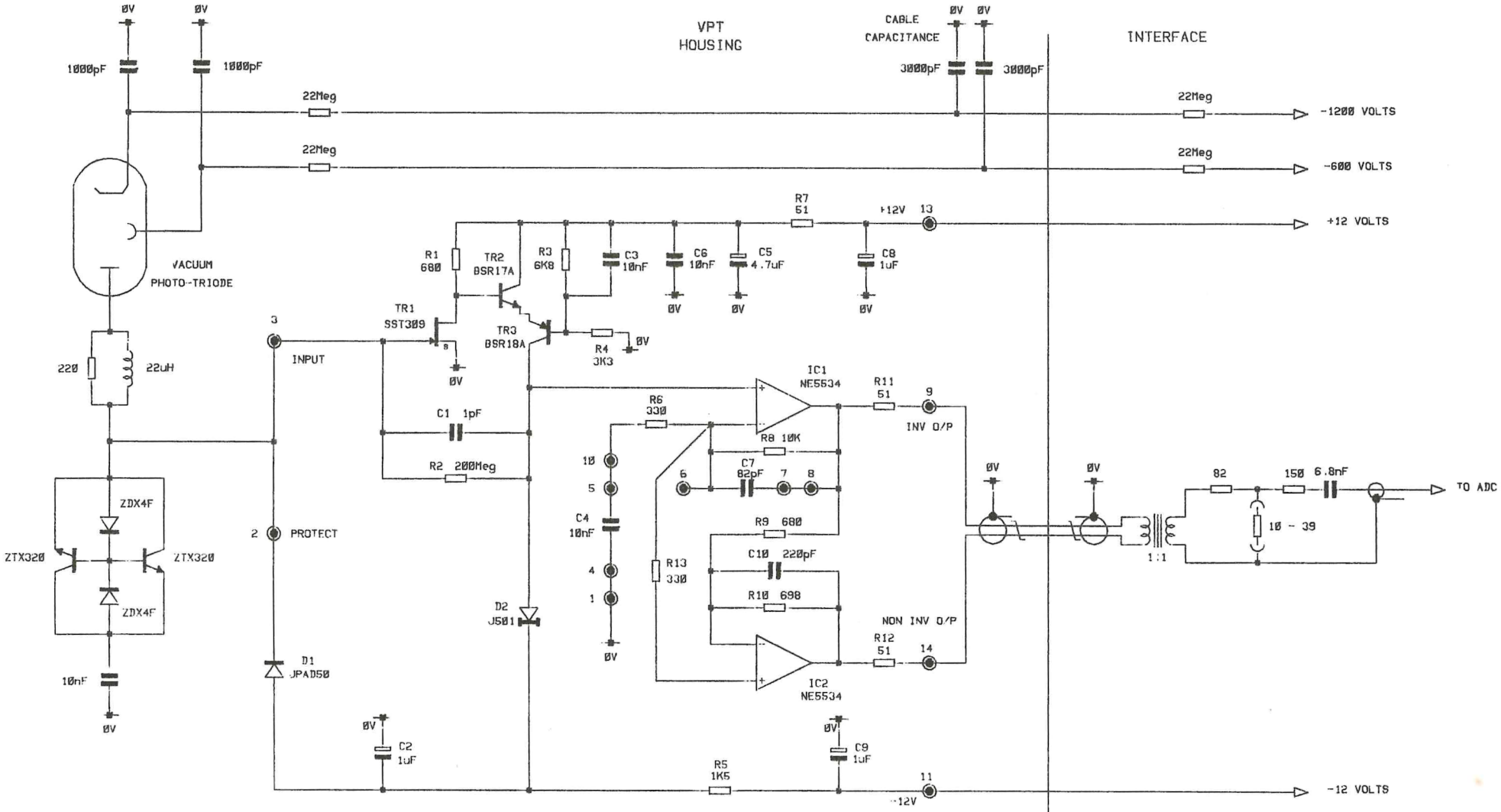
VPT
HOUSING
CABLE
CAPACITANCE
INTERFACE
ØV
1000pF
22Meg
-1200 VOLTS
-600 VOLTS
+12 VOLTS
VACUUM
PHOTO-TRIODE
220
22uH
INPUT
PROTECT
ZDX4F
ZTX320
10nF
D1
JPAD50
D2
J501
TR1
SST309
TR2
BSR17A
TR3
BSR18A
R1
680
R2 200Meg
R3
6K8
R4
3K3
C1 1pF
C2
1uF
C3
10nF
C4
10nF
C5
4.7uF
C6
10nF
C8
1uF
C9
1uF
R5
1K5
R6
330
R7
51
+12V
-12V
IC1
NE5534
IC2
NE5534
R8 10K
R9 680
C7
82pF
C10 220pF
R10 698
R11
51
R12
51
R13
330
INV O/P
NON INV O/P
82
150
6.8nF
10 - 39
1:1
TO ADC

FIGURE 3

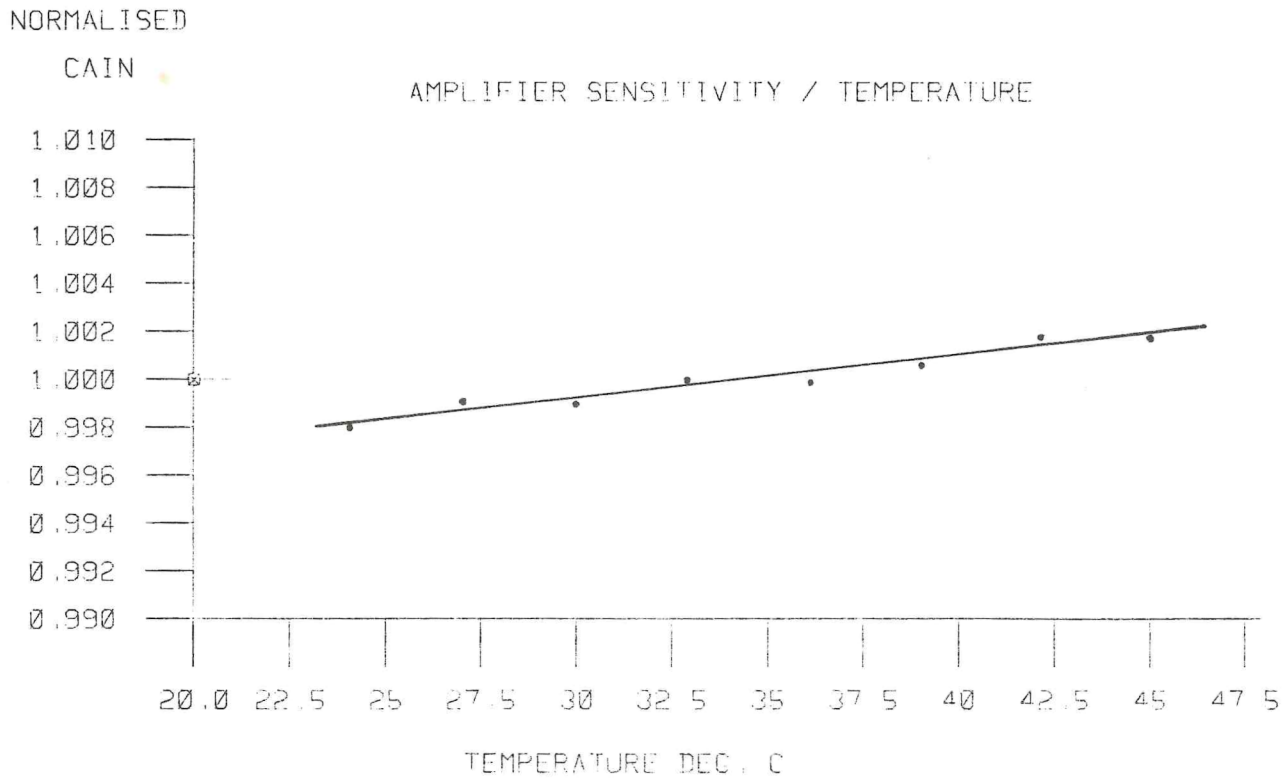

FIGURE 4

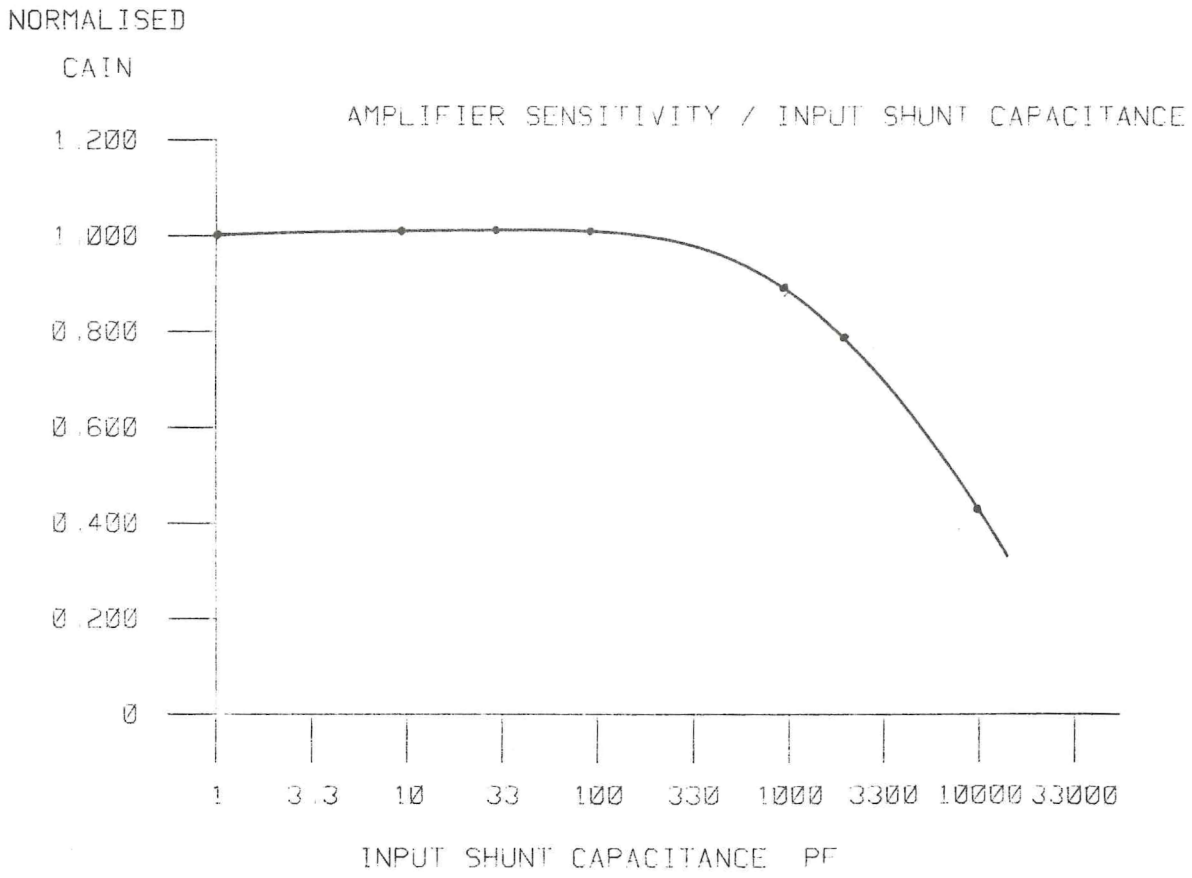

FIGURE 5

MAXIMUM OUTPUT INTO 50 OHMS

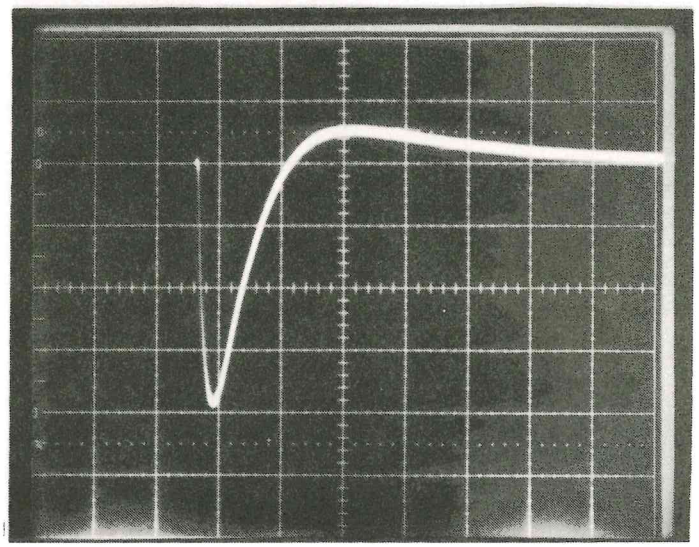

500 MILLI VOLTS / DIV

5 MICRO SECONDS / DIV

FIGURE 6

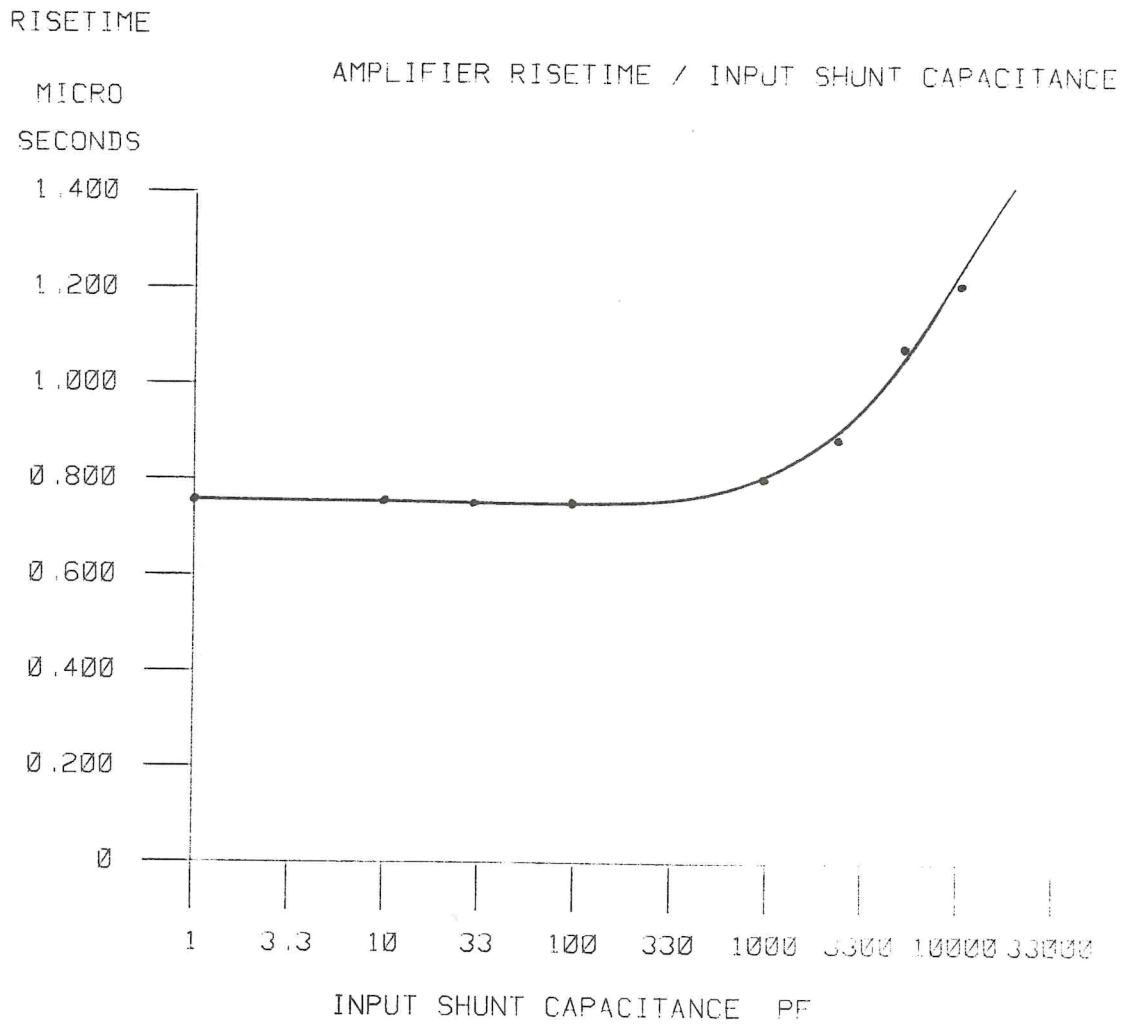

FIGURE 7

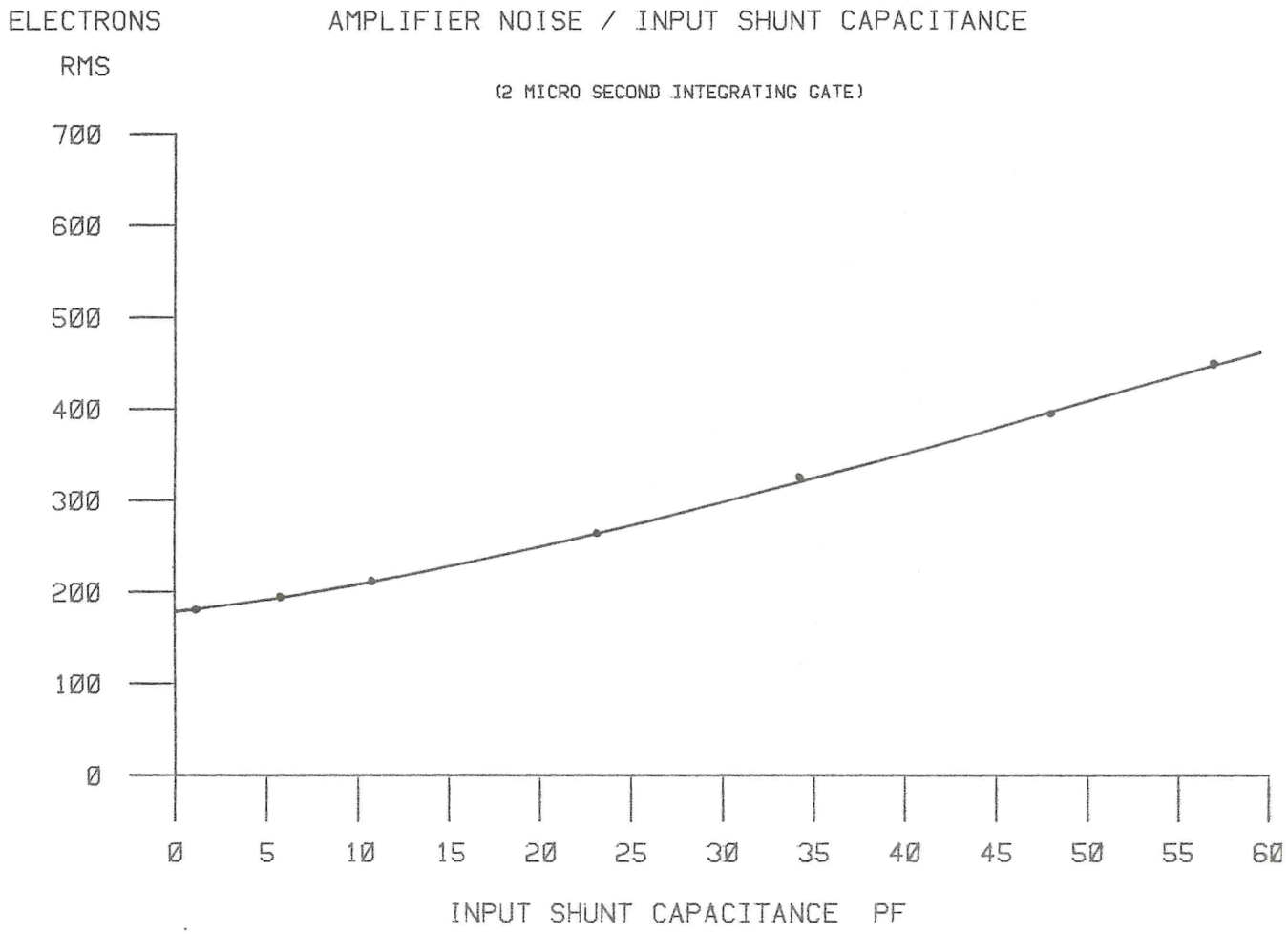

FIGURE 8

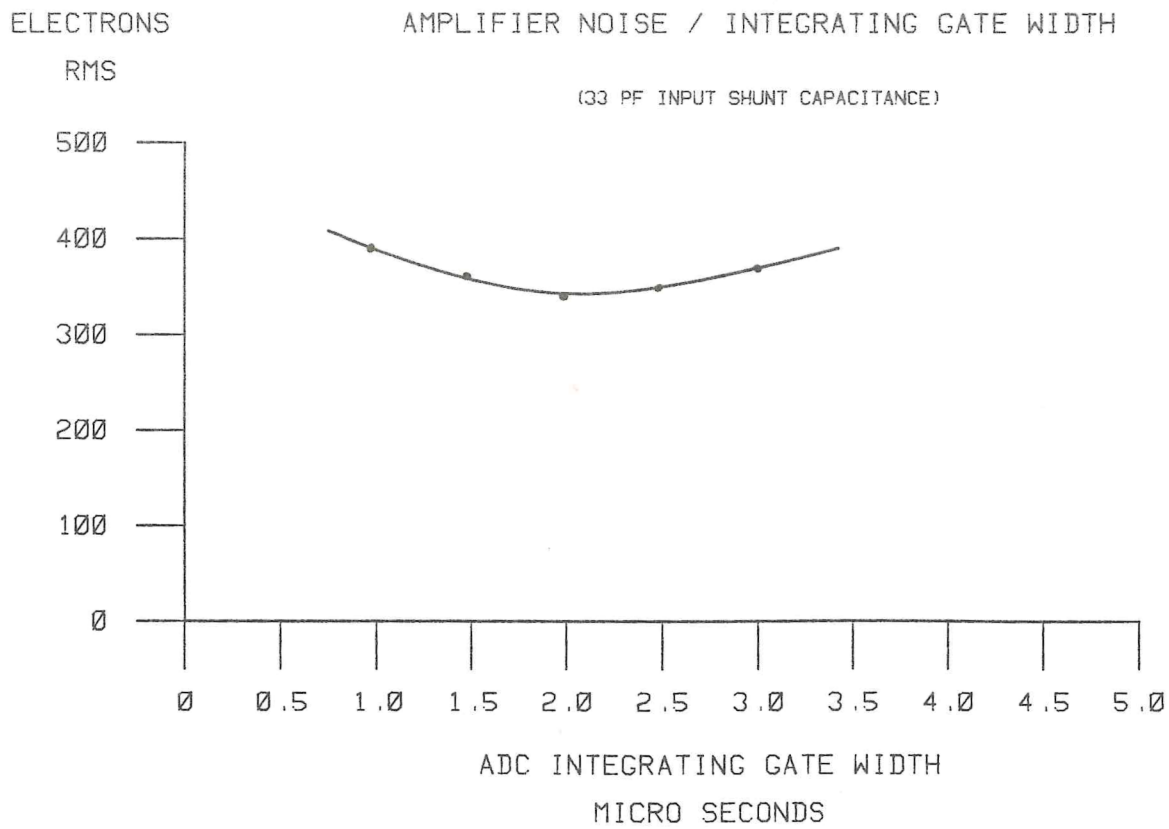

FIGURE 9

FREQUENCY PROFILE OF AMPLIFIER NOISE

33 PF INPUT SHUNT CAPACITANCE

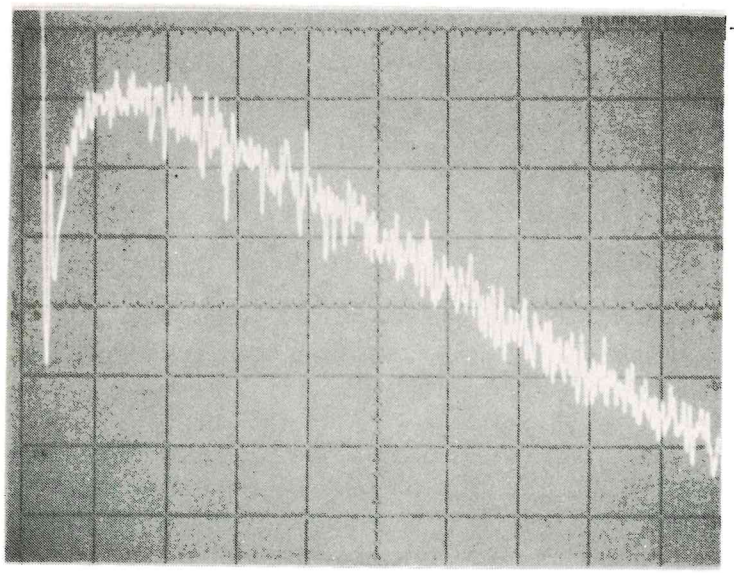

31.58 MICRO VOLTS

1 DB / DIV

3 KHZ RESOLUTION BANDWIDTH

Ø HZ

LINEAR

500 KHZ

FIGURE 10

AMPLIFIER RECOVERY CHARACTERISTIC

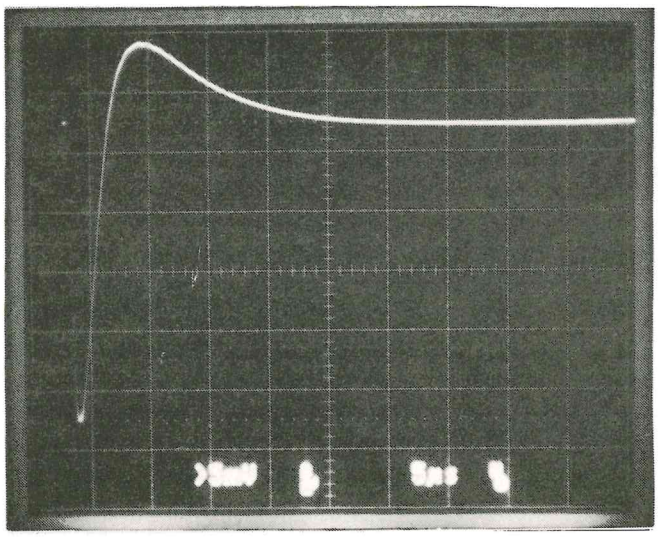

5 MILLIVOLTS / DIV

5 MICRO SECONDS / DIV

< 1% RESIDUAL AFTER 22 MICRO SECS.

FIGURE 11

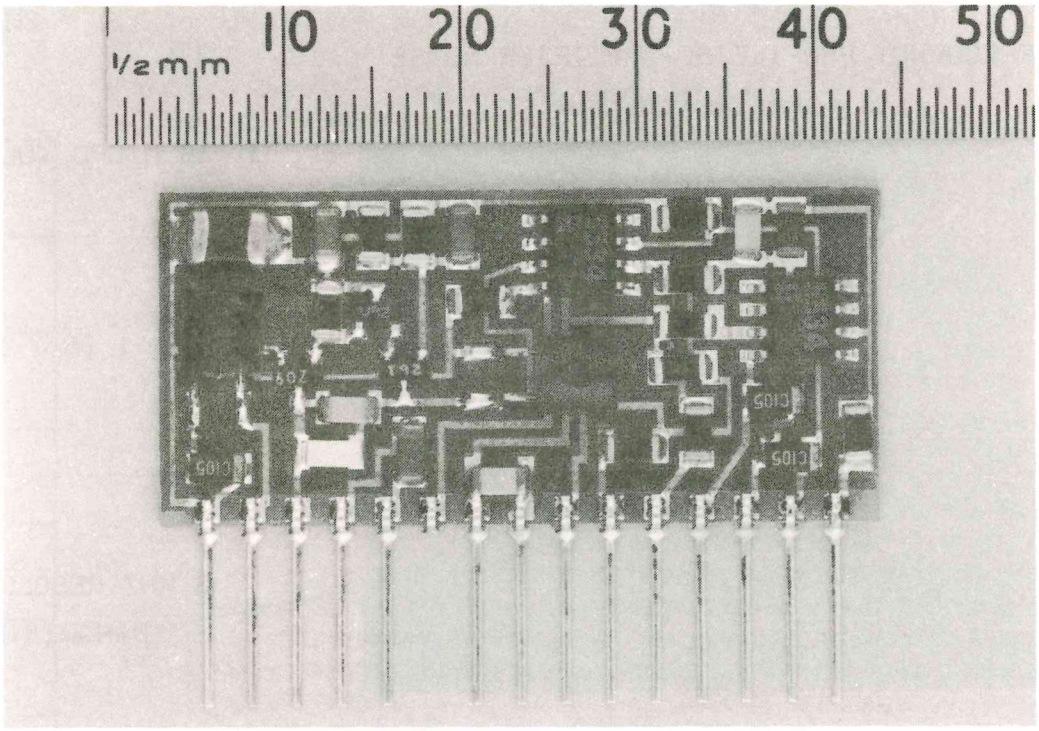

VIEW OF SURFACE MOUNTED PREAMPLIFIER

FIGURE 12

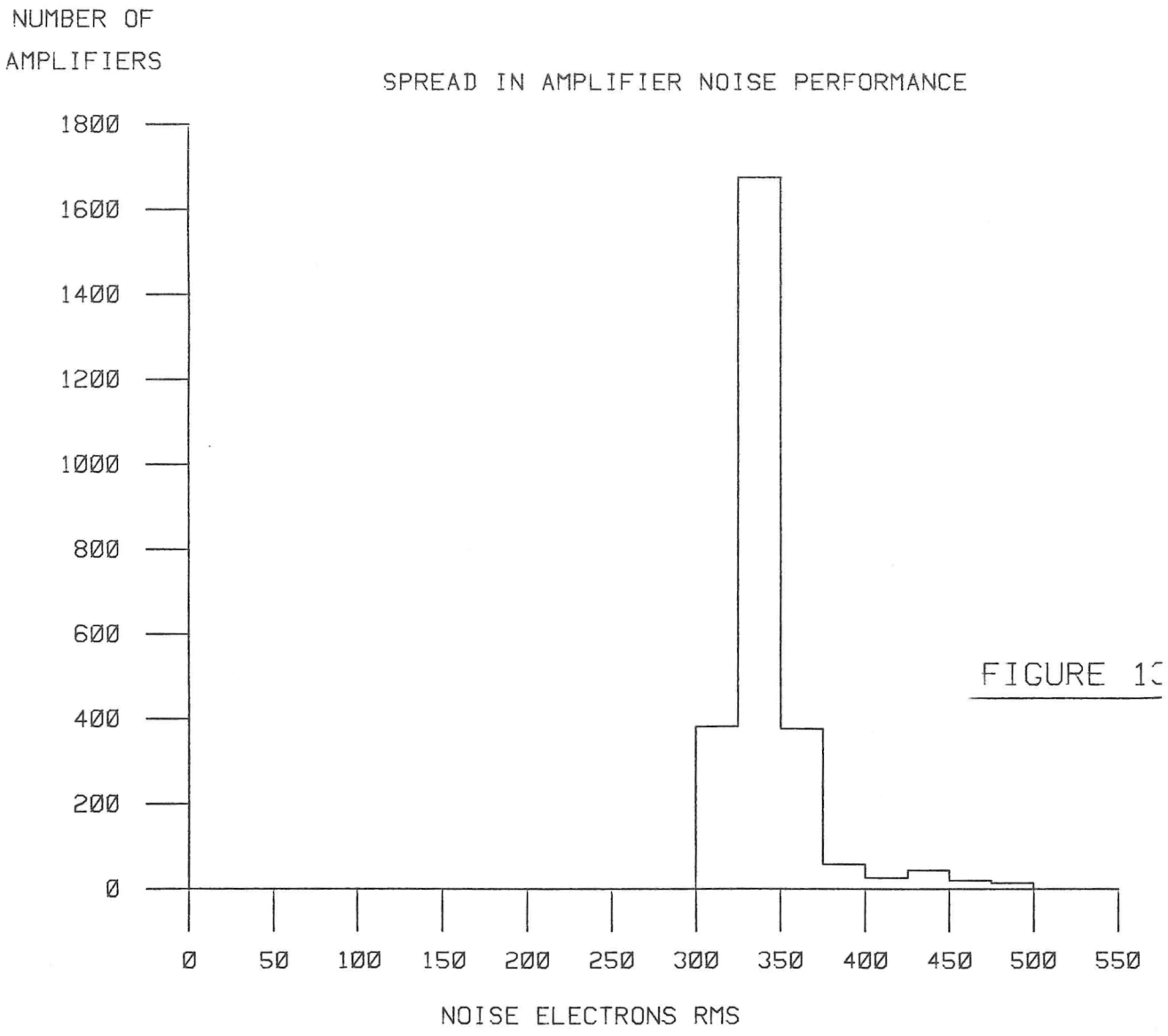

FIGURE 13

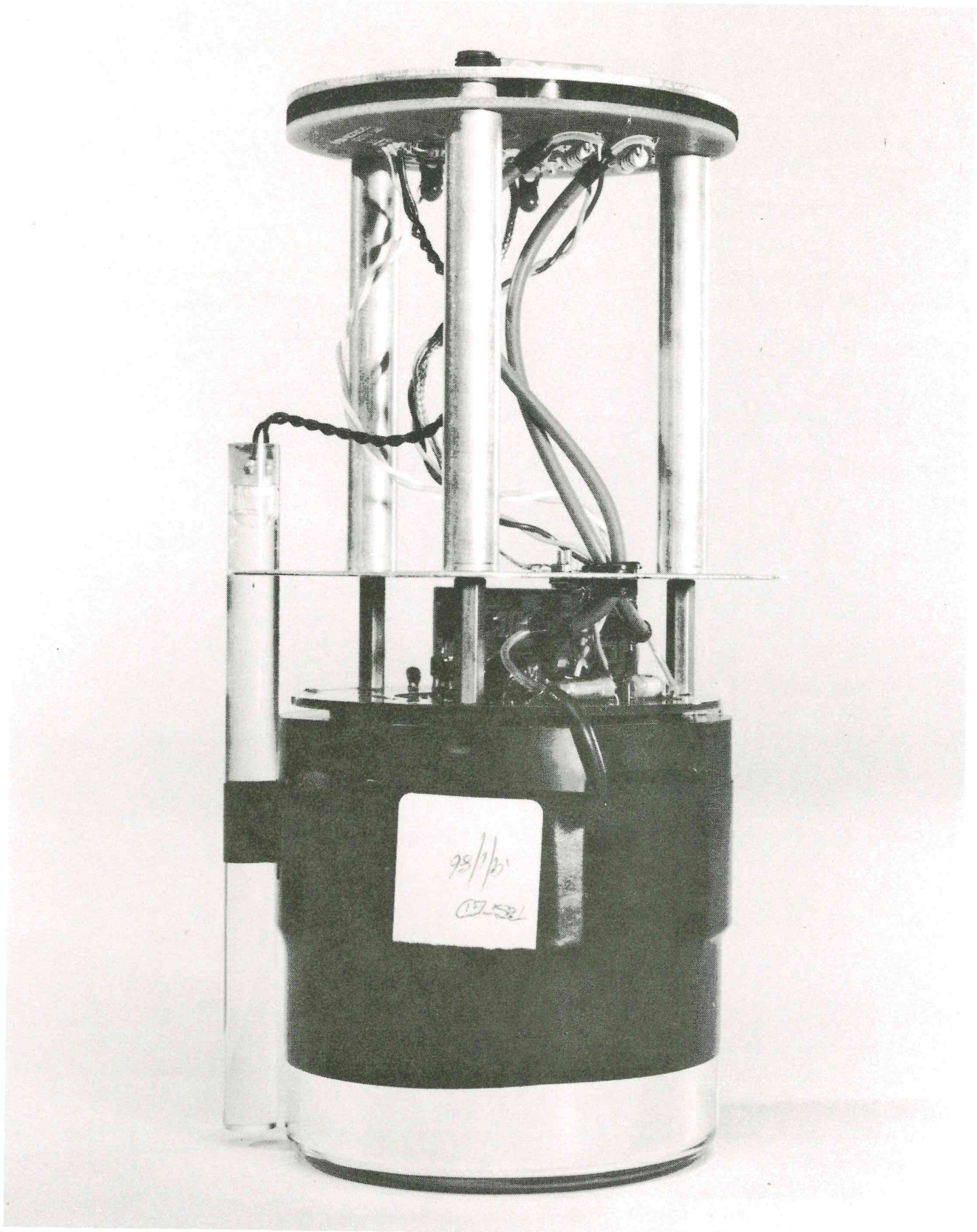

VIEW OF COMPLETE VPT HOUSING INTERNAL ASSEMBLY

FIGURE 14